Piece-wise partial matching of non-rigid shapes

Jan Hurtado-Jauregui
Pontifícia Universidade Católica do Rio de Janeiro
Rio de Janeiro, Brazil
jjauregui@inf.puc-rio.br

Abstract

Partial matching is one of the most challenging problems in shape analysis. Even, a more challenging problem arises when working with non-rigid shapes. This problem was addressed in different ways, but in this paper we are considering solve it as a multi-criterion optimization problem. We use a Mumford-Shah functional approximation generalized for surfaces, with integration of local descriptors as similarity criteria. In fact, we propose an extension of a previous work, reducing the dimensionality of the optimization problem. We use a subspace parametrization based on the Laplace-Beltrami operator. We show our solution in a continuous setting and its respective discretization. Also, we explain our experiments and give some conclusions.

1. Introduction

Shape analysis of deformable three-dimensional shapes (non-rigid shapes) has an important role in numerous applications related to pattern recognition, computer vision, geometry processing, and computer graphics. Similarity and correspondence finding are fundamentals problems inside this area, which are in most cases, previous problems to solve another problem. The main difficulty in the non-rigid realm, stems from the fact that the geometry is not preserved due to non-rigid transformations (e.g. isometric transformations). In addition to this difficulty, shapes can suffer perturbations such as gaussian noise, shot noise, topological noise, holes, global scale, local scale or sampling. For these reasons, it is common to use robust local intrinsic shape descriptors to address the mentioned problems.

A more challenging problem arises when we want to match an incomplete shape (subset of an unknown complete shape) to a transformation of the full version of this shape, i.e. a *part-in-whole* matching [7]. The phenomenon of incomplete shapes occurs, for example, when acquiring 3D scenes using range sensing devices, such as Microsoft Kinect, Intel RealSense camera or Project Tango device (Google). This happens due to partial view or occlusion.

In the case of rigid shapes, several methods based on variants of iterative closest point (ICP) algorithm, were proposed to solve the problem of shape matching [12, 4, 22, 16]. Using these kind of methods, the problem of partial matching can be addressed rejecting the points with bad correspondence [1, 2]. To avoid problems with the irregularity and the size of the resulting match, and following the spirit of the Mumford-Shah functional [23], A. Bronstein and M. Bronstein proposed in [5] the control of these variables using the ICP algorithm for the data term. This approach is a particular setting of the framework introduced in [9].

On the other hand, early methods tried to solve the problem of partial matching of non-rigid shapes, using local rigid shape matching. For example, in [19], Li *et al.* proposed to find an initial rigid alignment and then align not matched regions in the following steps. Based on the notion of Gromov-Hausdorff distance, Bronstein *et al.* proposed a generalization of a multidimensional scaling algorithm (GMDS), using minimum distortion correspondence [11]. Their framework is useful for global and partial matching problems.

A different class of methods, address this problem defining a multi-criterion optimization problem. In the case of two-dimensional shapes, Bronstein *et al.* proposed to maximize similarity and size of matched regions [8]. Following this idea, in [5], the authors argued that not only size matters, therefore, they included regularity as a significance criteria. Their approach follows the Mumford-Shah spirit, as in the rigid shape case. In [10], Bronstein *et al.* included statistical ocurrence of local shape descriptors as a significance criteria. Based on these ideas, an algorithm that generalizes them, was proposed in [9]. Consequently, Rodola *et al.* relaxed the optimization problem using sparse correspondence [27, 28].

Recently, van Kaick *et al.* introduced a local shape descriptor, which is robust for partial shape matching [32]. Sahillioglu and Yemez used a voting-based formulation to match shape extremities [30]. They consider that these extremities are preserved in the transformations. Brunton *et al.* proposed an alignment of tangent spaces, using a pre-

computed set of correspondences. In [29], Rodola *et al.* proposed an extension of *functional maps* framework [24], for partial correspondence. They used a similar regularization model used in [9]. Moreover, another methods, which consider the partial matching problem, work using collections of shapes [17, 13].

The aforementioned methods are based on the notion of point-wise correspondence. In contrast, Pokrass *et al.* presented an approach for correspondence-less partial matching of non-rigid shapes [25, 26], which was inspired in a work of partial matching of images [14]. They used the integration of local descriptors as a similarity criteria, and a regularization based on the Mumford-Shah functional. In spite of their method does not compute a point-wise correspondence, the proposed optimization problem depends on the number of sampled points. For this reason, the optimization scheme is very expensive.

In this paper, we present an extension of the above framework. We propose to reduce the dimensionality of the optimization scheme, using a subspace parametrization based on the Laplace-Beltrami operator. The solution is presented in a continuous setting, and then in a discrete setting. It is important to highlight that we use the same discretization proposed by Pokrass *et al.* [25, 26]. Our approach reduces significantly the dimensionality of the optimization problem and nearly preserves the matching of non-parametrized way.

The rest of the paper is structured as follows. In Section 2, we explain some concepts about the Laplace-Beltrami operator and the local descriptor we used (Heat Kernel Signature). Section 3 explains how to address the problem of partial matching, and how to reduce the dimensionality of the optimization problem. In Section 4 we show how to discretize the solution. Section 5 describes our implementation. In Section 6, we present our experimental results. And, finally, Section 7 concludes the paper.

2. Background

2.1. Laplace-Beltrami operator

The Laplace operator (Laplacian) is a second order differential operator which determines the divergence of the gradient of a function, in a n-dimensional euclidean space. It is defined as the sum of second order of partial derivatives, and can be denoted by:

$$div\ \nabla f = \Delta f = \nabla^2 f = \nabla \cdot \nabla f\ = \sum_{i=1}^{n} \frac{\partial^2 f}{\partial x_i^2}.$$

Intuitively, the Laplacian determines the irregularity of each point of a function, regarding a small neighborhood.

Using exterior calculus, the Laplacian definition can be generalized by a set of functions, defined on a manifold M equipped with a metric g. This generalization is called the Laplace-Beltrami operator, and it is defined as follows:

$$\nabla = \sum_i \frac{1}{\sqrt{|g|}} \frac{\partial}{\partial x_i} \sqrt{|g|} \frac{\partial}{\partial x_i},$$

where $|g|$ denotes the determinant of the metric g, and the term $\sqrt{|g|}$ can be interpreted as a local scale influenced by the element area.

Suppose that (M, g) is a complete Riemannian manifold, and g a Riemannian metric, the Laplace-Beltrami operator ∇ can be decomposed in eigenvalues $\{\lambda_n\}$ and eigenfunctions $\{\Phi_n\}$, such that $\nabla\Phi_n = -\lambda_n\Phi_n$. If the Laplace-Beltrami operator basis $\{\lambda_n\}$ is orthonormal, we can use it to represent any function defined on the manifold.

2.2. Heat Kernel Signature

The heat difussion over non-euclidean domains, is defined by the following equation:

$$\Delta_M u(x,t) = -\frac{\partial u(x,t)}{\partial t}, \tag{1}$$

where Δ_M is the Laplace-Beltrami operator for a manifold M, and $u(x,t)$ is the heat equation, which represent the heat distribution at point x at time t.

Given an initial distribution $f : M \to \mathbb{R}$, the heat operator $H_t(f)$ satisfies the heat equation for all t and it is defined as follows:

$$H_t f(x) = \int_M k_t(x,y) f(y) dy, \tag{2}$$

where $k_t(x,y)$ is the minimal function that satisfies the equation, and it is called heat kernel. If we define $H_t = e^{-t\Delta_M}$, the eigenfunctions of Δ_M and H_t will be the same. Also, $e^{-\lambda t}$ will define the eigenvalues of H_t, where λ represents the eigenvalues of Δ_M.

The heat kernel represents the amount of heat transferred from a point x to a point y. Its decomposition [18] is defined by:

$$k_t(x,y) = \sum_{i=0}^{\infty} e^{-\lambda_i t} \phi_i(x) \phi_i(y), \tag{3}$$

where λ and ϕ denotes the eigenvalues and eigenfunctions of Δ_M, and $\lambda_i \leq \lambda_{i+1}$.

The heat kernel $k_t(x,x)$ expresses the probability density of heat remaining at a point x after a time value t, and sometimes it is referred as the auto-diffusivity function. Sun *et al.* [31] and Gebal *et al.* [15] proposed point-wise descriptors, called heat kernel signatures (HKS), based on the discrete auto-diffusivity function regarding different time scales.

We use these descriptors as similarity features in our experiments, because they are robust regarding perturbations and discriminative.

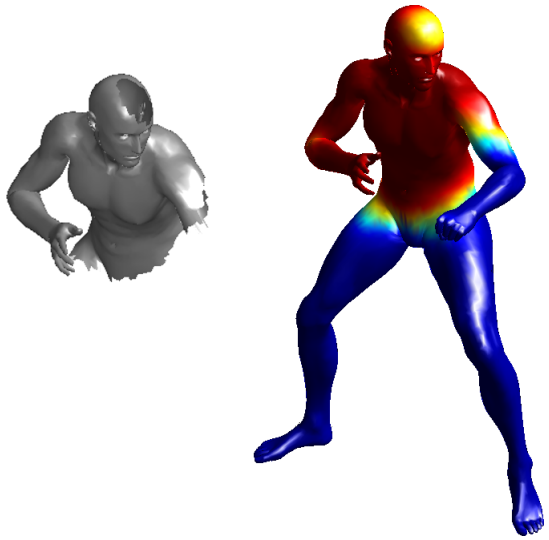

Figure 1: Example of membership function. Left: partial shape. Right: complete shape with membership values from 0 (blue) to 1 (red).

3. Partial matching

Given two shapes $Y' \subseteq Y$ and X, where Y is an unknown shape; we aim at finding a part $X' \subseteq X$, which is the most similar to Y'. To address this similarity, we define point-wise descriptors on both shapes, such that the integral of the descriptors computed on X' and Y', are as close as possible. Also, the area of X' must be equal to the area of Y'. To avoid fragmentation and irregularity problems, we have to penalize the boundary length of X'. Finding a crisp set X', that maximize the similarity between the integral of the descriptors and minimize the boundary length; results in an NP-hard combinatorial complexity problem. We relax the problem defining a fuzzy membership function u on X, instead of using a crisp set X'. This relaxation was proposed in [9, 5, 6]. The Ambrosio and Tortorelli aproximation of the Mumford-Shah functional on surfaces [3], allows us to define this optimization problem:

$$\min_{u,\rho} \left\| \int_X puda - \int_{Y'} qda \right\|^2 + \lambda_r R(u;\rho) \quad \text{s.t.} \quad \int_X uda = area(Y') \tag{4}$$

where p and q are the descriptor fields on X and Y' respectively, $u : X \to [0,1]$ is the membership function on X, and ρ is the phase field which indicates the discontinuity of u. The first term is the data term and the second one is the regularity term which influence is controlled by a parameter λ_r. The regularity term $R(u;\rho)$ is defined as follows:

$$\begin{aligned} R(u;\rho) = &\frac{\lambda_s}{2} \int_X \rho^2 \|\nabla u\|^2 da \\ &+\lambda_b \epsilon \int_X \|\nabla \rho\|^2 da \\ &+\frac{\lambda_b}{4\epsilon} \int_X (1-\rho)^2 da \end{aligned} \tag{5}$$

The smoothness of u is influenced by λ_s and the boundary length of u is influenced by λ_b. When $\epsilon \to 0$ the regularization converges to the crisp set defined previously ($\epsilon > 0$).

3.1. Alternating minimization

To simplify the optimization problem, we use alternating minimization. In the first step we fix ρ and solve:

$$\min_u \left\| \int_X puda - \int_{Y'} qda \right\|^2 + \lambda_r \frac{\lambda_s}{2} \int_X \rho^2 \|\nabla u\|^2 da \quad \text{s.t.} \quad \int_X uda = area(Y') \tag{6}$$

In the second step we fix u with the result in the previous step, and solve:

$$\begin{aligned} \min_\rho &\frac{\lambda_s}{2} \int_X \rho^2 \|\nabla u\|^2 da \\ &+\lambda_b \epsilon \int_X \|\nabla \rho\|^2 da \\ &+\frac{\lambda_b}{4\epsilon} \int_X (1-\rho)^2 da \end{aligned} \tag{7}$$

These steps are repeated iteratively. In the first iteration we initialize $\rho = 1$ according to Tikhonov regularization.

Unfortunately the complexity of the optimization problem depends on the number of sampled points of X. We propose reduce this complexity using a subspace parametrization.

3.2. Subspace parametrization

Given an orthonormal basis $\{\phi\}_{i \geq 1}$ defined on X, it is possible to represent any function $f : X \to \mathbb{R}$ as a linear combination of the bases:

$$f = \sum_{i \geq 1} c_i \phi_i \quad \text{s.t.} \quad c_i = \langle f, \phi_i \rangle$$

According to the latter, functions can be approximated using only k bases. So, $u : X \to \mathbb{R}$ and $\rho : X \to \mathbb{R}$ can be represented as follows:

$$u \approx \sum_{i=1}^{k} \alpha_i \phi_i, \quad \rho \approx \sum_{i=1}^{k} \beta_i \phi_i \tag{8}$$

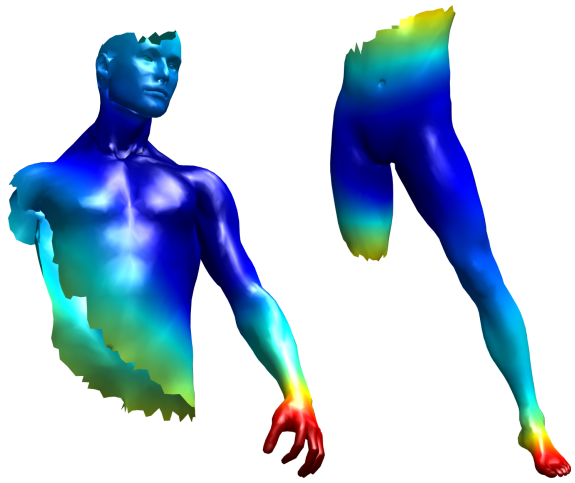

Figure 2: Boundary effects resulting after computation of a single time scale of the heat kernel signatures.

That allows us to solve the optimization problem over the coefficients instead of the functions, and now the minimization problem complexity depends on k. The new constraints are continue depending directly on u and ρ respectively. We show in Figure **??** an example of how a membership function looks like. The membership value goes from blue (0) to red (1).

4. Discretization

Our discretization is based on [25, 26]. We represent a 2-manifold as a triangular mesh in a R^3 space, such that each vertex of the triangulation represent a sampled point. Let us denote the sampled points as $X = \{x_1, \ldots, x_m\}$, and its respective functions u and ρ denoted by the vectors $\mathrm{u} = \{u_1, \ldots, u_m\}^T$ and $\rho = \{\rho_1, \ldots, \rho_m\}^T$ respectively. Also we define a vector $\mathrm{a} = \{a_1, \ldots, a_m\}$ which determines the area of each vertex. The areas are computed using barycentric area. Then, we define the matrix $A = diag\{\mathrm{a}\}$ as a diagonal $m \times m$ matrix, containing the defined areas.

Given the descriptor fields p and q of dimension d, defined on the target shape and the partial shape respectively, we represent them as matrices. $P_{d\times m}$ and $Q_{d\times n}$ are now the descriptor representations, where m is the number of points in the target shape and n is the number of points in the partial shape. The point-wise descriptors are stored in columns. It is possible to write the integral of the descriptor in this way:

$$\int_X puda \approx PA\mathrm{u}$$

$$\int_{Y'} qda \approx QA'1_n$$

where A' is a diagonal $n \times n$ matrix which contains the areas of the vertices in Y', and 1_n is a $n \times 1$ matrix of ones.

To simplify notation we define $\bar{\mathrm{q}} = QA'1_n$. This term is constant on each iteration of the optimization. Now, the data term can be discretized as follows:

$$\|PA\mathrm{u} - \bar{\mathrm{q}}\|^2 = \mathrm{u}^T A^T P^T PA\mathrm{u} - 2\bar{\mathrm{q}}^T PA\mathrm{u} + \bar{\mathrm{q}}^T\bar{\mathrm{q}} \quad (9)$$

We can ignore $\bar{\mathrm{q}}^T\bar{\mathrm{q}}$ in the minimization problem, because it's a constant.

For the regularization term, we have to compute the intrinsic gradient. The gradient flow on i^{th} point can be represented as a $2 \times m$ matrix G_i, such that $\nabla uda \approx G_i\mathrm{u}$. Considering all points of the shape, we have:

$$\int_X \rho^2\|\nabla u\|^2 da \approx \sum_{i=1}^{m} \frac{\rho_i^2}{a_i}\mathrm{u}^T G_i^T G_i\mathrm{u} \quad (10)$$

Defining the $2m \times m$ matrix G:

$$G = \left(diag\left\{\frac{1}{\sqrt{a_m}}, \ldots, \frac{1}{\sqrt{a_1}}\right\} \otimes I\right)\begin{pmatrix} G_1 \\ \vdots \\ G_m \end{pmatrix} \quad (11)$$

Thus, we can rewrite:

$$\begin{aligned}\int_X \rho^2\|\nabla u\|^2 da &\approx \|(diag\{\rho\} \otimes I)G\mathrm{u}\|^2 \\ &= \mathrm{u}^T G^T(diag\{\rho^2\} \otimes I)G\mathrm{u}\end{aligned} \quad (12)$$

where I is the 2×2 identity matrix.

With this terms we can define the first step of the minimization problem:

$$\begin{aligned}\min_{\mathrm{u}}\ &\mathrm{u}^T(A^T P^T PA + G^T(diag\{\rho^2\} \otimes I)G)\mathrm{u} \\ &-2\bar{\mathrm{q}}^T PA\mathrm{u} \quad s.t. \quad \mathrm{a}^T\mathrm{u} = area(Y')\end{aligned} \quad (13)$$

Using a truncated basis represented by the matrix Φ_k, where the columns are the sampled bases, we can approximate u:

$$\mathrm{u} \approx \Phi_k\alpha$$

where α is a vector that represent the truncated basis coefficients for u. Now, we can rewrite this step:

$$\begin{aligned}\min_{\alpha}\ &\alpha^T\Phi_k^T(A^T P^T PA + G^T(diag\{\rho^2\} \otimes I)G)\Phi_k\alpha \\ &-2\bar{\mathrm{q}}^T PA\Phi_k\alpha \quad s.t. \quad \mathrm{a}^T\Phi_k\alpha = area(Y')\end{aligned} \quad (14)$$

We have to define a non-negativity constraint and an upper bound constraint (≤ 1) for $\Phi_k\alpha$.

In the second step, we fix u and optimize over ρ. We can write

$$\begin{aligned}\int_X \rho^2\|\nabla u\|^2 da &\approx \sum_{i=1}^{m} \rho_i^2 \frac{1}{a_i}\mathrm{u}^T G_i^T G_i\mathrm{u} = \sum_{i=1}^{m} \rho_i^2 s_i \\ &= \rho^T diag\{s_1, \ldots, s_m\}\rho = \rho^T S(\mathrm{u})\rho\end{aligned} \quad (15)$$

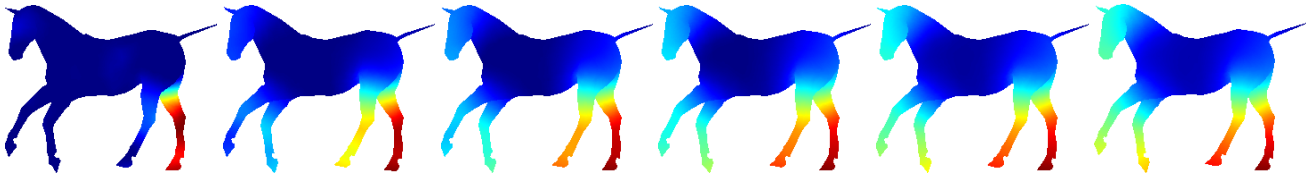

(a) $\lambda_r = 1$ (b) $\lambda_r = 100$ (c) $\lambda_r = 200$ (d) $\lambda_r = 300$ (e) $\lambda_r = 400$ (f) $\lambda_r = 500$

Figure 3: Influence of term λ_r

where $S(u)$ is diagonal matrix which contains the gradient norm of u. Then

$$\int_X \|\nabla\rho\|^2 da \approx \|G\rho\|^2 = \rho^T G^T G\rho \tag{16}$$

Finally,

$$\int_X (1-\rho)^2 da \approx \rho^T A\rho - 2\mathrm{a}^T\rho + 1_m^T\mathrm{a} \tag{17}$$

Now, we can define the minimization problem:

$$\min_\rho \rho^T\left(\frac{\lambda_s}{2}S(\mathrm{u}) + \lambda_b\epsilon G^T G\frac{\lambda_b}{4\epsilon}A\right)\rho - \frac{\lambda_b}{2\epsilon}\mathrm{a}^T\rho \tag{18}$$

In the same way like in the previous step, we can use the same basis to represent ρ:

$$\rho \approx \Phi_k\beta$$

where β are the truncated basis coefficients for ρ. Rewriting, we have:

$$\min_\beta \beta^T\Phi_k^T\left(\frac{\lambda_s}{2}S(\mathrm{u}) + \lambda_b\epsilon G^T G\frac{\lambda_b}{4\epsilon}A\right)\Phi_k\beta - \frac{\lambda_b}{2\epsilon}\mathrm{a}^T\Phi_k\beta \tag{19}$$

It is necessary to control the implicit constraints, non-negativity and upper bound, for u and ρ. These constraints are: $\Phi_k\alpha \in [0,1]$ and $\Phi_k\beta \in [0,1]$.

5. Implementation

To achieve the subspace parametrization, we need an orthonormal basis defined on the manifold, i.e. on a triangular mesh. We obtain this basis using a discrete representation of the Laplace-Beltrami operator [21], which defines cotangent weights to describe the connectivity of the vertices instead of regular values. Given two connected vertices v_i and v_j, the cotangent weight is defined as follows.

$$\delta_i = \frac{1}{|\Omega_i|}\sum_{j\in N(i)}\frac{1}{2}(\cot\alpha_{ij} + \cot\beta_{ij})(v_i - v_j),$$

where $|\Omega_i|$ the Voronoi area at vertex v_i, and α_{ij} and β_{ij} the opposite angles of edge (i,j). Following this idea, the

Algorithm 1 Partial matching algorithm

function MATCH($X, P, Y', Q, \lambda_r, \lambda_b, \lambda_s, \epsilon$)
- u[]= 0
- ρ[] = 1
- AX=area(X)
- AY'=area(Y')
- $\bar{q} = Q(AY')1_n^T$
- $tH1 = (AX)^T P^T P(AX)$
- $fz = (-2\bar{q}^T P(AX))\Phi$
- G = computeGradientFlow(X)
- **for** $i = 0$ to $num\_iterations$ **do**
  - $tH2 = \lambda_r\lambda_s\frac{1}{2}G^T(diag\{\rho^2\}\otimes I)G$
  - $H = \Phi^T(tH1 + tH2)\Phi$
  - z = quadraticOptimization(H,fz,constraints)
  - $u = \Phi z$
  - S = computeS(G,u)
  - $rH = \Phi^T((\frac{\lambda_s}{2})S + (\lambda_b\epsilon)(G^TG) + (\frac{\lambda_b}{4\epsilon}))(AX))\Phi$
  - $rfy = -((\frac{\lambda_b}{(2\epsilon)})diag(AX)^T)\Phi$
  - y = quadraticOptimization(rH,rfy,constraints)
  - $\rho = \Phi y$
- **end for**
- Return u

end function

Laplacian matrix can be expressed as $L = A^{-1}W$. Where A represents the diagonal matrix whose values determine the Voronoi area of each vertex. The weight matrix W is defined as follows.

$$(W)_{ij} = \begin{cases} \sum_{k\in N(i)} w_{ik} & i = j \\ -w_{ij} & (i,j)\text{is an edge} \\ 0 & \text{otherwise} \end{cases},$$

where $w_{ij} = \frac{\cot\alpha_{ij} + \cot\beta_{ij}}{2}$. The decomposition of this matrix give us an orthonormal basis.

The heat kernel signatures are computed using the latter definition of the Laplace-Beltrami operator. We used increasing time values trying to avoid boundary effects.

The algorithm for partial matching computation, receives as input the complete shape (X), the partial shape Y', the descriptors of both shapes (P and Q), and the regularity variables of the Mumford-Shah functional ($\lambda_r, \lambda_b, \lambda_s, \epsilon$).

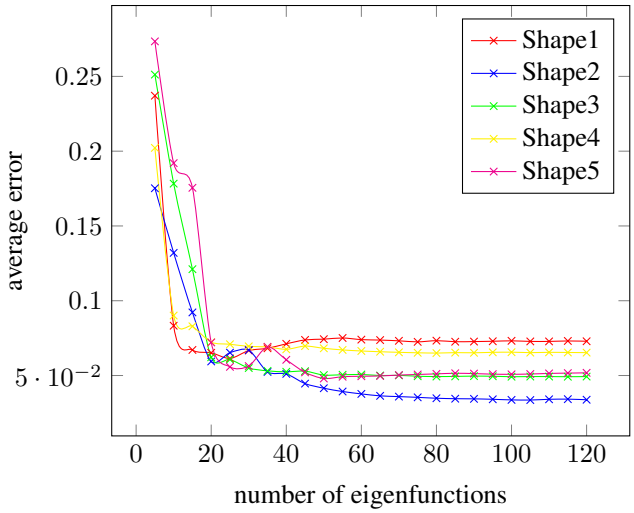

Figure 4: Convergence of the subspace parametrization evaluated on 5 random partial shapes. x axis represent the number of eigenvalues and y axis the average error regarding the partial matching without the parametrization.

The returning value is the membership function of the shape X. We present the pseudocode of this step in Algorithm 1.

6. Experiments and results

First of all, we should take care about which descriptor we select, the similarity criteria in the optimization problem depends on how discriminant is it. Another important feature is the descriptor's robustness regarding perturbations caused by meshing artifacts. For these reasons, we selected a collection of heat kernel signatures as descriptor. One of the problems that this descriptor presents, happens when the values near the boundary are calculated (See Figure 2). Due to the mesh structure, the decomposition of the Laplacian suffers distortions on these regions. To address this problem we can discard boundary points and a small neighborhood of them, and work only with the other points. Also, we can choose optimal time scales, such that the descriptor should not be strongly affected by the boundaries.

The regularization term is controlled by the variable λ_r, which is influential in the behavior of the resulting membership function. Using a shape of a horse as complete shape and its respective right back leg as partial shape, we computed the membership function resulting of the partial shape matching. In Figure 3, we show how the membership functions behaves when λ_r is incremented. For too high values, the match does not converge to a single compact shape. When λ_r is too low the optimization takes more time and the membership function is very irregular.

We use the proposed subspace parametrization with Φ_k as the first k eigenvectors of the Laplace-Beltrami operator decomposition (sorted in ascending order according to their respective eigenvalues). Regarding the number of eigenvectors (x axis), we can see the error between normal and parametrized optimization of some examples, in Figure 4. The average k for error convergence is when $k = 60$. The mesh has 2000 vertices, so, k represent 3% of the number of vertices.

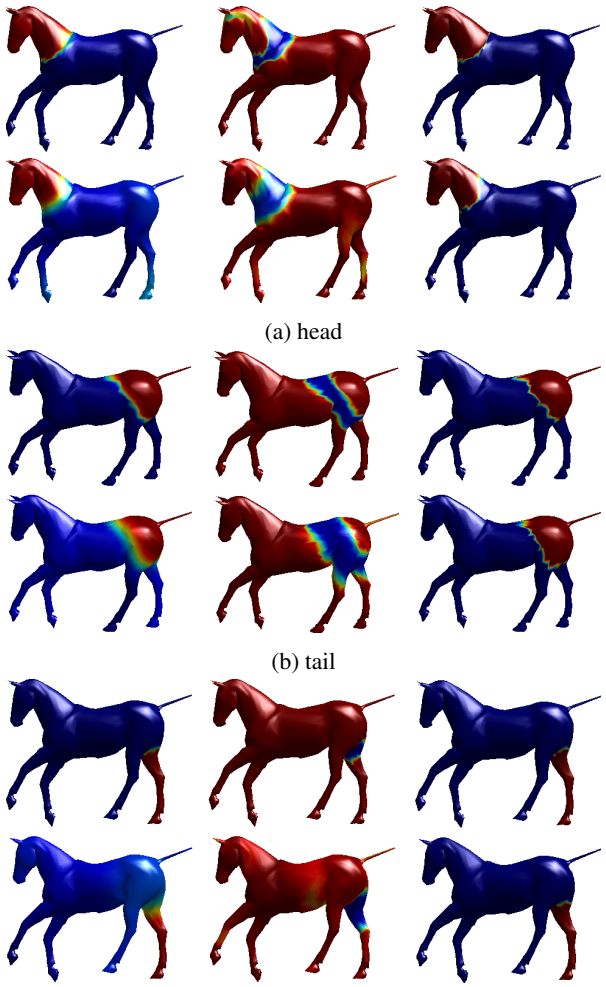

(a) head

(b) tail

(c) leg

Figure 5: Resulting match with three different partial shapes. First row: Pokrass *et al.* approach. Second row: our approach. First column: membership function. Second column: phase field. Third column: thresholded membership function.

In Figure 5, we show the behavior of the parametrization for 3 arbitrary partial shapes: head, tail and leg. Each subfigure describes the following. The first row represents the resulting functions of Pokrass *et al.* approach. The second row represents our results after the parametrization. The first column is the computed membership function and

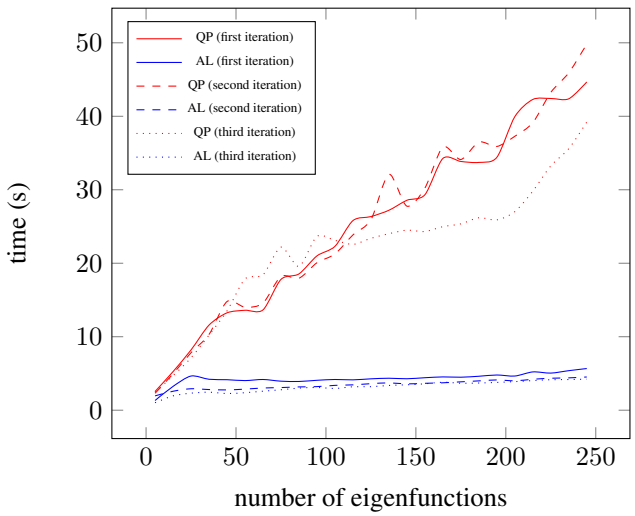

Figure 6: Execution time in seconds of partial matching using Quadratic Programming solver (QP) and Augmented Lagrangian solver (AL).

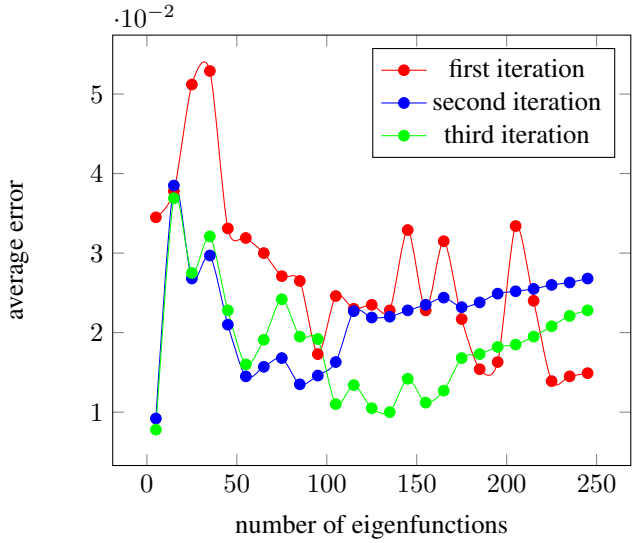

Figure 7: Average error when using Augmented Lagrangian solver.

the second one its respective phase field. The third column show the thresholded results. The values goes from 0 to 1, represented by color blue and red respectively.

Depending on the nature of our problem, we can choose the optimization method. In this work, we evaluated the resulting time in seconds using a Quadratic Programming solver and an Augment Lagrangian solver. In Figure 6 we show the resulting times for both methods, regarding the number of eigenvectors we choose. Also, in Figure 6, we present the resulting error between them. We can see that the Augmented Lagrangian solver improve the computation time of the Quadratic Programming method, and preserves a reasonable similarity (low error).

7. Conclusions and future work

We presented an extension of Pokrass *et al.* framework for partial shape matching [25, 26], implementing a subspace parametrization to reduce the dimensionality of the optimization problem. Our method nearly preserves the results of Pokrass *et al.*, and improve the computational complexity of their work.

The selection of the descriptor for the similarity criteria is very important. This descriptor should be discriminant strongly, robustness, and little affected by the boundary effects. The heat kernel signatures is a good choice in this sense, but we can test our results using others descriptors to obtain better results. The parameters of the regularization term are very important, because they control the compactness of the resulting match. An automatic selection of them, will depend on the scale of the input shapes and on the descriptor.

We proposed to represent the membership function using the Laplacian basis. This allows us to reduce the dimensionality of the variables in the optimization problem, but does not allows us to reduce the dimensionality of the constraints. We can get a truly k-dimensional optimization problem if we use an exponential function (e.g. $u \approx exp(-\Phi_k \alpha)$) or a sigmoid function with values between 0 and 1.

In the case of solver selection, we can include a column generation solver, because the values of the membership function, usually converges rapidly to 1 or 0.

This work can be extended for multi-part non-rigid shape matching, such as a non-rigid shape puzzle. In fact, Litany *et al.* proposed this idea in [20], using point-wise functional correspondences. As future work, we can address this problem too, finding piece-wise correspondences.

References

[1] D. Aiger, N. J. Mitra, and D. Cohen-Or. 4pointss congruent sets for robust pairwise surface registration. *ACM Trans. Graph.*, 27(3):85:1–85:10, Aug. 2008.

[2] A. Albarelli, E. Rodolà, and A. Torsello. Fast and accurate surface alignment through an isometry-enforcing game. *Pattern Recogn.*, 48(7):2209–2226, July 2015.

[3] L. Ambrosio and V. M. Tortorelli. Approximation of functional depending on jumps by elliptic functional via t-convergence. *Communications on Pure and Applied Mathematics*, 43(8):999–1036, 1990.

[4] P. J. Besl and H. D. McKay. A method for registration of 3-d shapes. *IEEE Transactions on Pattern Analysis and Machine Intelligence*, 14(2):239–256, Feb 1992.

[5] A. Bronstein and M. Bronstein. Not only size matters: Regularized partial matching of nonrigid shapes. In *Computer Vision and Pattern Recognition Workshops, 2008. CVPRW '08. IEEE Computer Society Conference on*, pages 1–6, June 2008.

[6] A. Bronstein and M. Bronstein. Regularized partial matching of rigid shapes. In D. Forsyth, P. Torr, and A. Zisserman, editors, *Computer Vision – ECCV 2008*, volume 5303 of *Lecture Notes in Computer Science*, pages 143–154. Springer Berlin Heidelberg, 2008.

[7] A. Bronstein, M. Bronstein, and R. Kimmel. *Numerical Geometry of Non-Rigid Shapes*. Springer Publishing Company, Incorporated, 1 edition, 2008.

[8] A. M. Bronstein, M. M. Bronstein, A. M. Bruckstein, and R. Kimmel. Analysis of two-dimensional non-rigid shapes. *Int. J. Comput. Vision*, 78(1):67–88, June 2008.

[9] A. M. Bronstein, M. M. Bronstein, A. M. Bruckstein, and R. Kimmel. Partial similarity of objects, or how to compare a centaur to a horse. *Int. J. Comput. Vision*, 84(2):163–183, Aug. 2009.

[10] A. M. Bronstein, M. M. Bronstein, Y. Carmon, and R. Kimmel. Partial similarity of shapes using a statistical significance measure. *IPSJ Transactions on Computer Vision and Applications*, 1:105–114, 2009.

[11] A. M. Bronstein, M. M. Bronstein, and R. Kimmel. Generalized multidimensional scaling: a framework for isometry-invariant partial surface matching. *Proceedings of the National Academy of Sciences*, 103(5):1168–1172, 2006.

[12] Y. Chen and G. Medioni. Object modeling by registration of multiple range images. In *Robotics and Automation, 1991. Proceedings., 1991 IEEE International Conference on*, pages 2724–2729 vol.3, Apr 1991.

[13] L. Cosmo, E. Rodolà, A. Albarelli, F. Mémoli, and D. Cremers. Consistent partial matching of shape collections via sparse modeling. 2016.

[14] C. Domokos and Z. Kato. *Affine Puzzle: Realigning Deformed Object Fragments without Correspondences*, pages 777–790. Springer Berlin Heidelberg, Berlin, Heidelberg, 2010.

[15] K. Gebal, J. A. Bærentzen, H. Aanæs, and R. Larsen. Shape analysis using the auto diffusion function. In *Proceedings of the Symposium on Geometry Processing*, SGP '09, pages 1405–1413, Aire-la-Ville, Switzerland, Switzerland, 2009. Eurographics Association.

[16] N. Gelfand, N. J. Mitra, L. J. Guibas, and H. Pottmann. Robust global registration. In *Proceedings of the Third Eurographics Symposium on Geometry Processing*, SGP '05, Aire-la-Ville, Switzerland, Switzerland, 2005. Eurographics Association.

[17] Q. Huang, F. Wang, and L. Guibas. Functional map networks for analyzing and exploring large shape collections. *ACM Trans. Graph.*, 33(4):36:1–36:11, July 2014.

[18] P. W. Jones, M. Maggioni, and R. Schul. Manifold parametrizations by eigenfunctions of the laplacian and heat kernels. *Proceedings of the National Academy of Sciences of the United States of America*, 105(6):pp. 1803–1808, 2008.

[19] H. Li, R. W. Sumner, and M. Pauly. Global correspondence optimization for non-rigid registration of depth scans. *Computer graphics forum*, 27(5):1421–1430, 2008.

[20] O. Litany, E. Rodolà, A. Bronstein, M. Bronstein, and D. Cremers. Non-rigid puzzles. 2016.

[21] M. Meyer, M. Desbrun, P. Schröder, and A. H. Barr. *Discrete Differential-Geometry Operators for Triangulated 2-Manifolds*, pages 35–57. Springer Berlin Heidelberg, Berlin, Heidelberg, 2003.

[22] N. J. Mitra, N. Gelfand, H. Pottmann, and L. Guibas. Registration of point cloud data from a geometric optimization perspective. In *Proceedings of the 2004 Eurographics/ACM SIGGRAPH Symposium on Geometry Processing*, SGP '04, pages 22–31, New York, NY, USA, 2004. ACM.

[23] D. Mumford. Optimal approximation by piecewise smooth functions and associated variational problems. *Commun. Pure Applied Mathematics*, pages 577–685, 1989.

[24] M. Ovsjanikov, M. Ben-Chen, J. Solomon, A. Butscher, and L. Guibas. Functional maps: A flexible representation of maps between shapes. *ACM Trans. Graph.*, 31(4):30:1–30:11, July 2012.

[25] J. Pokrass, A. Bronstein, and M. Bronstein. A correspondence-less approach to matching of deformable shapes. In A. Bruckstein, B. ter Haar Romeny, A. Bronstein, and M. Bronstein, editors, *Scale Space and Variational Methods in Computer Vision*, volume 6667 of *Lecture Notes in Computer Science*, pages 592–603. Springer Berlin Heidelberg, 2012.

[26] J. Pokrass, A. M. Bronstein, and M. M. Bronstein. Partial shape matching without point-wise correspondence. *Numerical Mathematics: Theory, Methods and Applications*, 6:223–244, 2 2013.

[27] E. Rodolà, A. M. Bronstein, A. Albarelli, F. Bergamasco, and A. Torsello. A game-theoretic approach to deformable shape matching. In *Computer Vision and Pattern Recognition (CVPR), 2012 IEEE Conference on*, pages 182–189, June 2012.

[28] E. Rodolà, A. Torsello, T. Harada, Y. Kuniyoshi, and D. Cremers. Elastic net constraints for shape matching. In *2013 IEEE International Conference on Computer Vision*, pages 1169–1176, Dec 2013.

[29] E. Rodolà, L. Cosmo, M. M. Bronstein, A. Torsello, and D. Cremers. Partial functional correspondence. *CoRR*, abs/1506.05274, 2015.

[30] Y. Sahillioğlu and Y. Yemez. Partial 3-d correspondence from shape extremities. *Computer Graphics Forum*, 33(6):63–76, 2014.

[31] J. Sun, M. Ovsjanikov, and L. Guibas. A concise and provably informative multi-scale signature based on heat diffusion. In *Proceedings of the Symposium on Geometry Processing*, SGP '09, pages 1383–1392, Aire-la-Ville, Switzerland, Switzerland, 2009. Eurographics Association.

[32] O. van Kaick, H. Zhang, and G. Hamarneh. Bilateral maps for partial matching. *Comput. Graph. Forum*, 32(6):189–200, Sept. 2013.